Review

Treatment Technology and Research Progress of Residual Xanthate in Mineral Processing Wastewater

Jiaqiao Yuan [1,2], Suqi Li [1], Zhan Ding [1,2], Jie Li [1,2], Anmei Yu [1,2], Shuming Wen [1,2,3] and Shaojun Bai [1,2,3,*]

[1] Faculty of Land Resource Engineering, Kunming University of Science and Technology, Kunming 650093, China
[2] State Key Laboratory of Complex Nonferrous Metal Resources Clean Utilization, Kunming University of Science and Technology, Kunming 650093, China
[3] Yunnan Key Laboratory of Green Separation and Enrichment of Strategic Mineral Resources, Kunming 650093, China
[*] Correspondence: baishaojun830829@126.com; Tel.: +86-871-65187288

Abstract: Xanthate is the most widely used and effective collector in the flotation of sulfide minerals. However, the residual xanthate in flotation wastewater may cause serious environmental pollution and even human health hazards. At present, a variety of treatment technologies have been developed to degrade xanthate pollutants in wastewater, with the aim of meeting safe discharge standards. This work reviews the research status of xanthate wastewater treatment technologies in recent years. Treatment technologies are evaluated, including coagulation flocculation, adsorption, microbiological, Fenton, ozone oxidation, and photocatalytic methods. The reaction mechanisms and advantages, as well as disadvantages, of the various treatment technologies are summarized. Future research on the treatment of xanthate wastewater should focus on combined methods, which will be conducive to achieving a high efficiency and low cost, with no secondary pollution, and with the aim of generating further original and innovative technologies.

Keywords: flotation wastewater; residual xanthate; treatment technology; catalytic oxidation methods

1. Introduction

Recently, environmental issues related to the mineral processing industry have received increased attention from researchers. The efficient treatment of mineral processing wastewater is the focus of research in this field. It is well accepted that froth flotation, on the basis of the different surface properties of minerals, has become the most common and effective beneficiation method for separating metallic sulfide minerals from the gangue [1]. It is statistically estimated that approximately 2 billion tons of minerals are processed by flotation methods every year [2], which mainly involves copper, lead, zinc, nickel, etc. Xanthate is the most widely used agent in the flotation of non-ferrous metal sulfide minerals, and its consumption is expected to reach about 371,826,000 tons by 2025 [3]. However, only half of the xanthate in the flotation process is consumed, while the remainder is discharged to the tailings pond [4,5]. The residual xanthate wastewater can leak out and cause odor problems and toxicity to the biota, resulting in the deterioration of the surrounding water quality [6]. When recycling the beneficiation wastewater, this remaining agent will affect the flotation index and cause adverse effects on the flotation selectivity of the minerals [7]. Thus, effective treatment of the residual xanthate in flotation wastewater is of great significance to the sustainable development of the mineral processing industry and for environmental protection.

Various methods have been reported for the treatment of xanthate wastewater [8], primarily including acid decomposition and conventional chemical oxidation. The conventional chemical oxidizing agents mainly consist of hydrogen peroxide (H_2O_2) and hypochlorite (NaClO, $Ca(ClO)_2$, etc.). However, there are still many issues with these
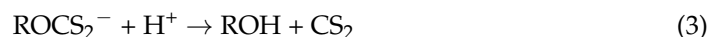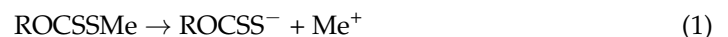
traditional processes. For instance, a continuous supply of chemicals and energy are required when acid decomposition methods are employed. Therefore, most of them are both unaffordable and unsustainable [9]. The conventional chemical oxidation methods have an extremely low treatment efficiency, and the treated xanthate wastewater cannot meet emission standards for release into the environment, which can produce secondary pollution [10]. Therefore, it is vitally important to develop effective methods with higher oxidation capacity, with the aim of better removal of xanthate.

In order to overcome the shortcomings of these traditional treatment methods, researchers have developed techniques such as physical adsorption [7,11], coagulation flocculation [12], and microbiological methods [4,13]. They exhibit superior performance for the treatment of xanthate wastewater, due to the advantages of simple operation and relatively mature technology. During the last few decades, efforts for the treatment of mineral processing wastewater via advanced oxidation processes (AOPs) have been ongoing. Photocatalytic [14,15], ozone oxidation [16], and Fenton [17,18] are frequently cited as the prime examples of such processes. They become effective alternative methods for degrading residual xanthates in flotation wastewater, because of a high xanthate removal rate, short treatment duration, as well as no secondary pollution. With the ever-increasing raising of environmental protection requirements, the development of efficient treatments for xanthate wastewater has become a hot topic, and our goal is to summarize the recent advances in the treatment of xanthate wastewater, and to guide the future utilization of wastewater resources and environmental protection.

In view of this, the aim of this review is to critically analyze the broad-spectrum treatment methods that have been engaged in the published literature on the degradation of xanthate wastewater. The reaction mechanisms and related influencing factors of the various treatment techniques for the removal of xanthate are explored, while the characteristics and hazards of xanthate are briefly discussed. Finally, updated applications for the removal of residual xanthate from flotation wastewater are emphasized. A review such as this will help researchers understand the progress in research, identify the strengths and weaknesses of each treatment technology, and document knowledge gaps that could help shape the direction of future studies in this area.

2. The Characteristics and Hazards of Xanthate

Xanthate is chemically formulated as ROCSSMe (Me is Na and K). It is easily decomposed and has good water solubility [19]. It can be partially degraded naturally under light conditions, and is unstable under strong acid, strong alkali, as well as neutral conditions [20,21]. In the water system, a series of chemical reactions, as shown in Equations (1)–(4), occur, leading to the decomposition of xanthate [20].

$$ROCSSMe \rightarrow ROCSS^- + Me^+ \tag{1}$$

$$ROCSS^- + H_2O \rightarrow ROCSSH + OH^- \tag{2}$$

$$ROCS_2^- + H^+ \rightarrow ROH + CS_2 \tag{3}$$

$$ROCSSH \rightarrow ROCSS^- + H^+ \tag{4}$$

In acidic solutions, xanthate is readily decomposed into alcohols and carbon disulfide (CS_2):

$$ROCSS^- + H^- \rightarrow ROCSSH \tag{5}$$

$$ROCSSH + H^- \rightarrow ROCSSH_2^+ \tag{6}$$

$$ROCSSH \rightarrow ROH + CS_2 \tag{7}$$
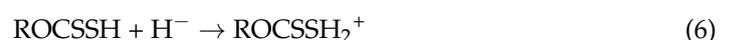
In alkaline solutions, xanthate is readily oxidized to dixanthate and further converted to alcohols and carbon disulfide (CS2) in contact with air:

$$2ROCSS^- + 1/2O_2 + H_2O \rightarrow (ROCSS)_2 + 2OH^- \tag{8}$$

$$ROCSS^- + CO_2 + H_2O \rightarrow ROH + CS_2 + HCO_3^- \tag{9}$$
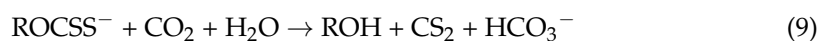
Xanthate and its derivatives are highly toxic and difficult to degrade. Once the xanthate wastewater enters a water body, even in very small amounts, it can cause water quality deterioration and a bad smell, as well as affect the growth and reproduction of algae, fish, and microorganisms in the water [22,23]. It has been reported that 30 μg/L of xanthate had a significant disruptive effect on the embryonic development of salmonids [24]; 19.25 mg/L of xanthate had a dramatic inhibitory effect on chlorella pyrenoidosa [25]. In addition, xanthate can have a negative impact on the nervous system and liver of humans and animals [26,27]. In addition, xanthate easily forms complex pollutants once it interacts with heavy metals, accelerating the migration, transformation, and residence time of heavy metal elements in the environment [25,28]. This activity can cause inhibition of enzymatic activities, genetic mutations, and chromosomal mutations in organisms [29], making the toxicity of xanthate wastewater more serious.

3. Xanthate Wastewater Treatment Technology

3.1. Coagulation–Flocculation Method

Coagulation–flocculation is an effective method that is widely used to remove pollutants from wastewater. The mechanism is designed to allow polymerization sedimentation of organic pollutants, by adding coagulants and flocculants to the wastewater [30]. The commonly used coagulants are iron salts, ferrous salts, aluminum salts, and their polymers [31]. Polyacrylamides and their derivatives are frequently used as flocculants.

The xanthate anion can combine with many metal ions and readily forms salt species with a smaller solubility. Metal ions such as Fe^{2+}, Cu^{2+}, Pb^{2+}, and Cd^{2+} [32] are usually added to the xanthate wastewater to form metal xanthate precipitates, and the removal of xanthate and soluble contaminants can be achieved by filtration. $FeSO_4$, polymerized ferric sulfate (PFS), and polyacrylamide (PAM) were added to the wastewater containing high concentrations of xanthate by Sun et al. [33]. The removal of xanthate could reach more than 99% under neutral conditions. Meng et al. [31] indicated that the coagulation–flocculation process using polymerized ferric sulfate as a coagulant and polyacrylamide as a flocculant showed an insignificant removal effect in reducing COD (Chemical Oxygen Demand) in tailings wastewater. Yang et al. [30] reported that a coagulation–flocculation process was employed to treat flotation wastewater with a high concentration of suspended solids (SS) and organic pollutants, high alkalinity, and strong coloration, through the use of ferric chloride (FC) and polymerized aluminum chloride (PAC) as coagulants and polyacrylamide (PAM) as a flocculant. The results indicated that the FC/PAC compound coagulant coupled with PAM flocculant showed a high potential and economic feasibility for treating flotation wastewater with high turbidity and high alkalinity.

The coagulation–flocculation method has the advantages of simple operation and easy control. However, this treatment process requires a large amount of coagulants, making the cost high. In addition, the formation of a multitude sedimentation wastes can cause secondary pollution. In addition, this process is highly dependent on pH, which requires a large input of acid and alkali to adjust the solution pH. These drawbacks limit its application in the treatment of practical flotation wastewater.

3.2. Adsorption Methods

Adsorption is a simple, efficient, and economical method for removing residual xanthate from flotation tailings. The main technique is using adsorbents to separate the xanthates from the wastewater. The commonly used adsorbents include activated carbon, fly ash, zeolite, clay minerals, etc.

Activated carbon is effective as an adsorbent for the treatment of low concentration xanthate wastewater. Salarirad et al. [34] investigated the adsorption performance of ethyl xanthate (EX) in flotation wastewater using activated carbon. The results revealed that the removal rate of EX was more than 99% when the initial concentration of EX was 268 mg/L. Additionally, clay minerals and their modified forms have been widely
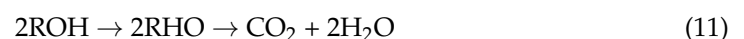
applied as adsorbents for the treatment of xanthate, due to their stable physicochemical properties, large specific surface area, rich pore structure, and surface properties. Huang et al. [35] used cationic gemini surfactant-modified montmorillonite for the removal of ethyl, isobutyl, and isoamyl xanthates, and the three xanthates were completely removed within 60 min. This result indicated that modified montmorillonite was a promising adsorbent for the removal of xanthate from solution, but its regeneration performance needs to be confirmed. In addition, it was shown by Oliveira et al. that zeolites pretreated with sodium ions and then modified with copper ions exhibited excellent adsorption properties for isopropyl xanthate [36].

It was found that bentonite showed good adsorption properties for the removal of xanthate. Amrollahi et al. [3] reported the adsorption characteristics of bentonite modified with copper-manganese ferrite nanoparticles (Be-CuFe$_2$O$_4$, Be-MnFe$_2$O$_4$) on synthetic and actual mine wastewater with xanthate, in which the removal rate of residual xanthate reached more than 94% under optimal adsorption conditions. Rezaei et al. [11] applied acid-activated (H-Be) and aluminum-pillared (Al-Be) bentonite and obtained two modified adsorbent materials, which were successfully used for the removal of residual potassium amyl xanthate from solution. The adsorption performance of Al-Be was superior to H-Be, and the removal rate of residual xanthate reached over 99%. Li et al. [37] investigated the adsorption of xanthate from aqueous solution using multilayer graphene oxide and obtained a desirable removal rate of xanthate. The superior adsorption performance was attributed to the abundant oxygen-containing functional groups and large specific surface area of the multilayer graphene oxide.

Although adsorbents are inexpensive and widely available, their adsorption capacity is limited. They are usually applied to treat low concentration xanthate wastewater. Adsorbent clogging is a prominent issue when treating high concentration xanthate wastewater. In addition, the issue of regeneration and reuse of adsorbents needs to be further explored.

3.3. Biological Method

Microbiological techniques have been widely used to remove organic pollutants from various types of wastewater. Biological treatment of xanthate wastewater is accomplished through the decomposition of xanthate into CO$_2$, CS$_2$, and dixanthate with the action of microorganisms [38]. The degradation mechanisms are as follows [39]:

$$8ROCSS^- + 4H_2O + O_2 \rightarrow 8ROH + 2CO_3{}^{2-} + 2CS_2 + 4CS_3{}^{2-} \tag{10}$$

$$2ROH \rightarrow 2RHO \rightarrow CO_2 + 2H_2O \tag{11}$$

$$CS_3{}^{2-} \rightarrow CS_2 + S^{2-} \tag{12}$$

$$2ROCSS \rightarrow (ROCSS)_2 \tag{13}$$

Chen et al. [38,40] found that domesticated microorganisms were beneficial for the biodegradation of xanthate. The results showed that the removal of xanthate reached 81.8% after 8 days of biodegradation, and the treatment process was consistent with the first order reaction kinetics. Furthermore, the biodegradation mechanism of xanthate revealed that CS$_2$, ROCSSH, and monothiolcarbonate were the main degradation products, accompanied by the generation of a small amount of dixanthate oil droplets. Natarajan et al. [4] demonstrated that paenibacillus polymyxa and pseudomonas putida had the ability to degrade isopropyl xanthate, but the xanthate exerted toxic effects on bacterial growth when the concentration of xanthate exceeded 50 mg/L. To overcome the above limitations, bacterial strains resistant to high concentrations of xanthate were cultivated by continuous subculture. The significant effect of this strain on the degradation efficiency of the xanthate was mainly attributed to the acidic products produced by the bacterial metabolism.

Lin et al. [41] reported that an artificial microbial community SDMC (simultaneously degrade butyl xanthate and biomineralize cadmium) composed of hypomicrobium and sporosarcina after screening and domesticating in a short period of time achieved 100%

butyl xanthate (BX) removal and 99% Cd biosorption, respectively. The main mechanisms of SDMC degradation and biomineralization of complex contaminants were attributed to decomposition, degradation, biomineralization, C-O bond breaking, and microbially induced carbonate precipitation (MICP) (as shown in Figure 1). In addition, CS_2, butyl perxanthate (BPX), and $(Ca_{0.67}, Cd_{0.33}) CO_3$ were the main products produced during the degradation of the composite pollution. Chockalingam et al. [42] reported the biodegradation of potassium isopropylxanthate in aqueous solution by bacillus polymyxa. Xanthate degradation product was observed at 1046 cm^{-1} via FTIR spectrum analysis, indicating the biodegradation mechanism. Cheng et al. [1] also designed an anaerobic–aerobic biological filter for the degradation of xanthate in synthetic flotation wastewater. As a result, an average COD removal rate of 88.7% for potassium ethyl xanthate was obtained under optimal reaction conditions, and a biological filter with volcanic rock as filler showed a favorable biodegradation performance for xanthate.
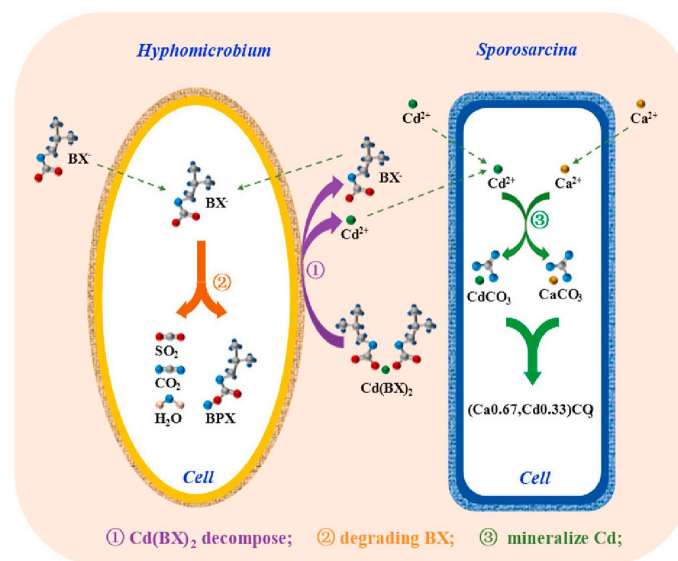

Figure 1. Degradation/biomineralization pathway sketch map (Reproduced from J. Environ. Manage. 2022, 316, 115304 with permissions from Elsevier, Netherlands) [41].

In view of their simplicity of operation, economy, and environmentally friendliness, researchers argue that biological methods are suitable for the treatment of xanthate wastewater [41]. However, this method also has defects, such as a low efficiency and long duration. In addition, the CS_2 and alcohols produced by the decomposition of the xanthate are toxic to bacterial growth and activity, which not only leads to an increase in the permeability of lipid membranes and the inability to carry out normal metabolism, but also triggers the secondary contamination of CS_2.

3.4. Oxidation Methods

Advanced oxidation processes (AOPs) are considered an effective and promising method for degrading refractory organic pollutants in wastewater. Many AOPs, such as ozone oxidation, Fenton oxidation, and photocatalytic oxidation have been widely used in the degradation of xanthates in mineral processing wastewater, due to their powerful oxidation capacities [43]. The reactive oxygen species (ROS) produced by the oxidation method, such as hydroxyl radicals ($\bullet$OH), sulfate radicals ($SO_4\bullet^-$), superoxide radicals ($O_2^-\bullet$), and hydroperoxyl radicals ($HO_2\bullet$) can oxidize organic pollutants into harmless small molecule compounds, in the form of CO_2 and H_2O [44,45]. Therefore, AOPs have great potential for the degradation of xanthate pollutants. The advantages and limitations of various AOPs are summarized in Table 1.

Table 1. The advantages and limitations of various AOPs.

AOPs	Advantages	Disadvantages
Fenton	• Rapid degradation rate • Mild reaction conditions • Convenient operation	• High dosage of reagents • Limited pH range • Catalysts are not easily recovered •Excess Fe^{2+} increases the color and COD of the treated water • Secondary pollution
Ozonation	• Short reaction time • High removal rate of xanthate	• Limited mass transfer efficiency and utilization productivity • High treatment costs •Low mineralization rate of the intermediates • Intermediate products increase the COD content of the effluent
Photocatalytics — TiO_2 photocatalysts	• Low cost • Innocuous and harmless • Strong redox capability • Excellent chemical stability	• Wide band gap • Electron-hole pairs are unstable • Narrow light absorption range • Low adsorption capacity •High concentration nano-TiO_2 suspensions are easy to agglomerate
Bi-based oxide photocatalysts	• Innocuous and harmless • Excellent chemical stability • Unique layered structure • Excellent photophysical properties	• Electron-hole pairs are unstable • Visible light absorption is limited to a specific wavelength range
ZnO-based photocatalysts	• Low cost • High light sensitivity and thermal stability	• Wide band gap • Photoinduced carriers are unstable • Low sunlight usage rate

3.4.1. Fenton Methods

In recent years, Fenton oxidation technology has been widely investigated in the wastewater treatment field. The Fenton method includes homogeneous Fenton and non-homogeneous Fenton, according to the catalyst used. In the conventional Fenton oxidation process, Fe^{2+} catalyzes the reaction of H_2O_2 under acidic conditions, to form hydroxyl radicals (•OH) [46,47]. The •OH has a high redox potential of 2.8 eV, which can effectively degrade most organic pollutants (e.g., xanthate) in wastewater [46,48]. The amount of •OH produced mainly depends on the concentration of Fe^{2+} and H_2O_2 in the solution system. An appropriate concentration of Fe^{2+} and H_2O_2 is beneficial for the generation of •OH, but excessive Fe^{2+} and H_2O_2 will consume the produced •OH, which degrades the activity of the Fenton reagent [49]. Thus, it is essential to determine the optimal ratio of Fe^{2+} and H_2O_2 for xanthate wastewater treatment.

Fenton oxidation was used to remove residual xanthate from sulfide ore beneficiation wastewater by Ai et al. [50]. Under optimal conditions, the removal of xanthate from both synthetic and actual beneficiation wastewater was extremely high and met the required discharge standards, where the maximum allowable concentration of xanthate is 0.005 mg/L according to the Comprehensive Sewage Discharge Standard (GB8978−1996) [51]. In the case of excess Fe^{2+}, H_2O_2 and Fe^{2+} were consumed rapidly and Fe^{3+} ions were formed, resulting in a change of the color of the treated water. Meanwhile, the efficiency of wastewater treatment decreased with a high initial pH. Based on this, another study by Ai et al. [19] reported the combination of ultrasound with a Fenton reagent. This combined process exhibited higher removal rates of xanthate wastewater. However, numerous inherent disadvantages exist of the conventional homogeneous Fenton reactions, such as strong acidic conditions and the production of iron sludge, which limit the wide application of the homogeneous Fenton method in wastewater treatment [52]. To further expand the applicability of the homogeneous Fenton method in the treatment of xanthate wastewater, shorten the reaction time, and improve the reaction efficiency, a non-homogeneous phase

Fenton-like method has been developed by researchers. The non-homogeneous Fenton-like reaction is a general term for a class of reactions in which Fe^{3+}, Fe-containing minerals, and other transition metals such as Co, Cd, Cu, Ag, Mn, Al, etc. accelerate or replace Fe^{2+} and catalyze H_2O_2 to produce active groups [53,54].

García-Leiva et al. [6] compared the effect of the Fenton process and a photo-Fenton process on the oxidative degradation of ethyl xanthate (EX) in aqueous solution. The results indicated that the photo-Fenton method could promote the complete mineralization of organic compounds and sulfur in xanthate, and its performance for EX removal was better than the conventional Fenton method. The potential application of acidified/calcined red mud (ACRM) as a catalyst of Fenton in the degradation of butyl xanthate was reported in another work [55]. The authors further explored the possible mechanisms of hydroxyl radical generation and butyl xanthate degradation in an ACRM-catalyzed Fenton-like process (as shown in Figure 2). The xanthate was first oxidized by ●OH radicals to produce peroxynitrite, and then continued to be oxidized to H_2O and CO_2, and finally the xanthate was effectively removed. Similarly, Chen et al. [17] discussed the removal of n-butylxanthate from an aqueous solution through a non-homogeneous Fenton-like method that utilized fly ash as a catalyst. UV-Vis spectroscopic analysis (Shimadzu, Japan) showed that CS_2 was the oxidation intermediate in the oxidation of n-butylxanthate. Under optimal test conditions, the xanthate and COD removal reached more than 96.90% and 96.66%, respectively. This result indicated the high oxidative activity of the process for the degradation of xanthate in aqueous solution.
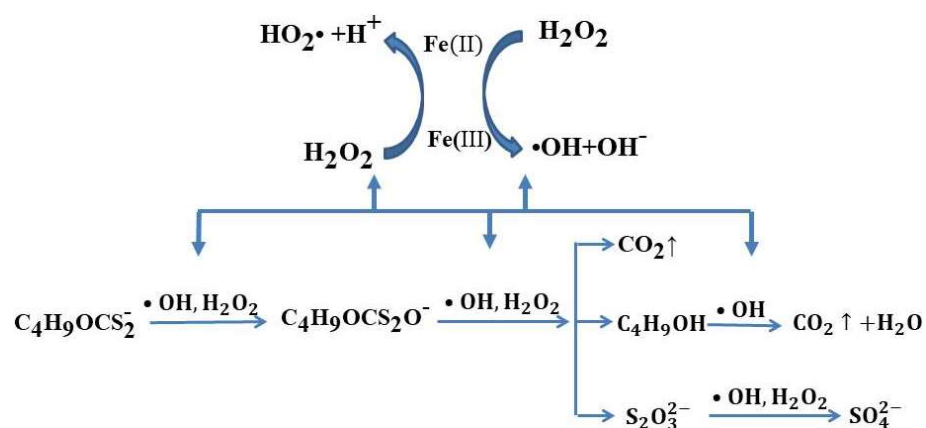

Figure 2. Production of hydroxyl radicals and degradation pathway of butyl xanthate (reproduced from Environ. Sci. Pollut. Res. Int. 2016, 23, 15202−15207 with permission from Elsevier) [55].

3.4.2. Ozone Oxidation

The oxidation potential of ozone is 2.07 eV. Therefore, ozone oxidation may also be very effective for the treatment of xanthate wastewater. The oxidation reaction of ozone is divided into two pathways: one is the direct oxidation of molecular ozone, the other is the indirect oxidation through its own decomposition to produce hydroxyl radicals (●OH) and other free radicals [56,57]. In this process, pH is the main factor that affects the effectiveness of the xanthate wastewater treatment. Under acidic conditions, the organic components in xanthate wastewater are directly oxidized by O_3; while in alkaline systems, xanthate is indirectly attacked by the highly oxidizing ●OH produced by the rapid reaction of O_3 with OH^-. However, ozone oxidation has the disadvantages of a limited mass transfer of ozone, short lifetime of the generated ozone and reactive oxygen species (ROS), and relatively high energy consumption of the ozone generated. Thus, its application in practical flotation wastewater treatment is limited [58]. In addition, it is difficult to completely oxidize and mineralize the toxic intermediates during the oxidation process through single O_3 oxidation [59]. To overcome these drawbacks, using ozone in combination with other processes to improve the O_3 oxidation efficiency has attracted a lot of attention from researchers. Current research on the treatment of xanthate using ozone has focused on

comparing the degradation performance of ozone and the synergistic effect of ozone with other advanced oxidation processes, the purpose of which is to develop a more effective treatment method for xanthate wastewater.

It has been shown that the COD removal and ozone utilization are quite limited when using a single ozone oxidation process in the degradation of butyl xanthate [60]. The combination of ozone oxidation and UV radiation (O_3/UV) is an effective combined process for the removal of refractory pollutants from wastewater [61]. Fu et al. [62] compared the performance of O_3 and UV-O_3 processes for the removal of four alkyl (sodium ethyl xanthate (SEX), sodium isopropylxanthate (SIPX), sodium n-butyl xanthate (SBX) and sodium namyl xanthate (SAX)) xanthates in a semi-batch bubble column reactor. Although UV spectral analysis showed that the ozone oxidation process had a high removal rate of alkyl xanthate in a short period of time, its mineralization effect was still unsatisfactory. On the contrary, the improvements in xanthate mineralization rate and ozone utilization in the UV/O_3 process were mainly attributed to the easy decomposition of O_3 under UV radiation, to form reactive radicals. In addition, a decomposition pathway of n-butylxanthate in the vacuum UV-ozone (VUV/O_3) process has been proposed (as shown in Figure 3) [16]. UV promoted the decomposition of refractory xanthates by generating more $\bullet$OH radicals. The C-O bond in the xanthate molecule was attacked by $\bullet$OH in aqueous solution and the C=S bond in the –CSS^- functional group was broken by nucleophilic reactions, to form by-products such as n-butanol and CS_2 [26]. These by-products were further attacked by $\bullet$OH, to form CO_2, H_2O, and SO_4^{2-}, with a smaller molecular mass. Fu et al. [63] compared the degradation performance of an ethyl xanthate (EX) collector using O_3, UV_{254nm}, $UV_{185+254nm}$, O_3/UV_{254nm}, and O_3/$UV_{185+254nm}$ processes. The O_3/$UV_{185+254nm}$ process showed the highest degree of removal and mineralization of xanthate. However, a solid-phase extraction/GC-MS (Shimadzu, GCMS–QP2010 SE, Japan) analysis showed that the EX collector produced 13 organic by-products, and most of them could be further decomposed by O_3/$UV_{185+254 nm}$, but there were still a few by-products that were difficult to completely mineralize. Yan et al. [64] analyzed in detail the decomposition pathway and final oxidation products of potassium n-butyl xanthate (PBX) removal through an ozone oxidation process. In the presence of ozone, the PBX was significantly degraded to SO_4^{2-} and n-butanol, accompanied by small amounts of carbon dioxide and gaseous sulfur. Direct and indirect ozone oxidation reactions occurred in the PBX solution. In the indirect ozone oxidation reaction of PBX, the continuous reactions between peroxide radicals ($\bullet HO_2$ and $\bullet O_2^-$) and PBX caused the decomposition of PBX into small organic and inorganic substances.

Figure 3. Decomposition pathway of n-butylxanthate in the VUV/O_3 process (reproduced from Process Saf. Environ. Prot. 2016, 102, 64−70 with permission from Elsevier) [16].

3.4.3. Photocatalytic Oxidations

TiO_2 Photocatalysts

Titanium dioxide (TiO_2) is the one of the most important semiconductor materials in the field of photocatalysis, because of its chemical stability, high catalytic activity, and non-toxicity. TiO_2 mainly includes three crystalline types: anatase phase, rutile phase, and

brookite phase [65]. The photocatalytic performance of anatase phase TiO_2 was more active than the other two crystalline TiO_2 types [66]. TiO_2 is an n-type semiconductor compound, and its photocatalytic mechanism is shown in Figure 4 [67]. When TiO_2 is irradiated in UV light with an energy (hv) greater than or equal to the band gap energy, the photogenerated electron (e^-) on its step band (vb) is transferred to the conduction band (cb). At the same time, photogenerated holes (h^+) are generated in the valence band, and the electron-hole pairs migrate to the semiconductor surface, under the action of the electric field [68]. The holes can directly oxidize the organic compounds that are adsorbed on the surface of the TiO_2. It can also react with H_2O molecules to produce hydroxyl radicals ($\bullet OH$) with an extremely high oxidizing power. Photogenerated electrons can reduce O_2 molecules, to form superoxide radical anions ($\bullet O_2^-$) or hydrogen peroxide radicals ($HO_2\bullet$), as shown in Equations (14)–(20) [69,70]. Organic pollutants are oxidized by these reactive oxygen species (ROS) to generate small molecule compounds, such as CO_2 and H_2O, thereby achieving a clean treatment of organic pollutants.

$$TiO_2 + hv \rightarrow h_{vB}^+ + e_{cB}^- \tag{14}$$

$$h_{vB}^+ + e_{cB}^- \rightarrow Energy \tag{15}$$

$$h_{vB}^+ + H_2O \rightarrow \bullet OH + H^+ \tag{16}$$

$$e_{cB}^- + O_2 \rightarrow \bullet O_2^- \tag{17}$$

$$\bullet O_2^- + H^+ \rightarrow HO_2\bullet \tag{18}$$

$$2HO_2\bullet + e_{cB}^- + H^+ \rightarrow H_2O_2 + O_2 \tag{19}$$

$$H_2O_2 + e_{cB}^- \rightarrow HO\bullet + HO^- \tag{20}$$
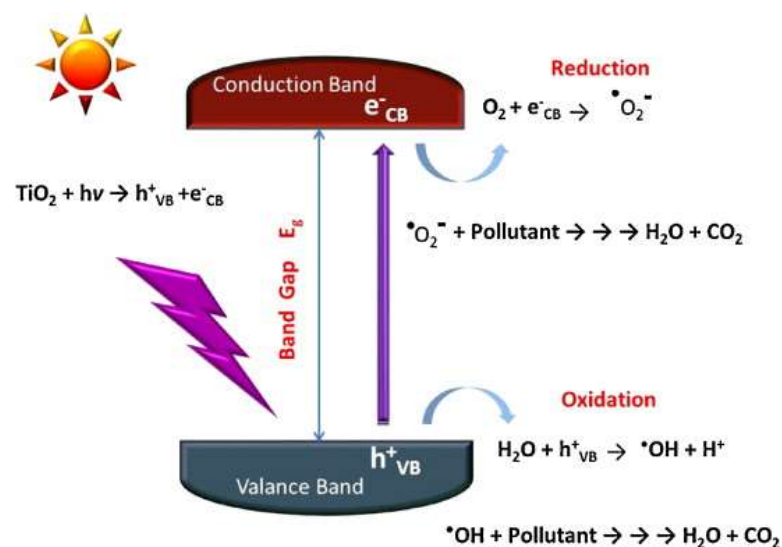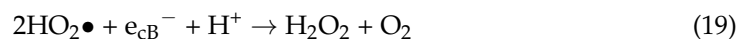
Figure 4. TiO_2 photocatalytic mechanism diagram [67].

However, pure TiO_2 photocatalysts usually exhibit a low photocatalytic efficiency because of their drawbacks, such as a wide band gap, partial absorption of sunlight in the UV region, and rapid recombination of the photogenerated electron-hole pair, which limit the practicality of pure TiO_2-based materials [71,72]. In addition, the low adsorption capacity and easy agglomeration of TiO_2 particles also limit their further application in the field of photocatalysis [73]. To enhance the photocatalytic activity, modification methods such as doping modification, photosensitization, and semiconductor coupling to form heterostructures have been extensively studied by researchers [74–76]. The degradation efficiency of different modified catalysts for xanthate was compared, as shown in Table 2.

Table 2. The degradation efficiency of different modified catalysts for xanthate.

Photocatalyst	Light Source	Pollutant	Synthesis Methods	Degradation (%)	Refs.
Ce/NeTiO$_2$@AC	Visible light irradiation	Sodium isobutyl xanthate	Sol-gel method	95.80	[77]
Ag-TiO$_2$-FAMB	Visible light irradiation	Sodium butyl xanthate	Sol-gel method	98.50	[14]
TiO$_2$/clinoptilolite	UV irradiation	Sodium isopropyl xanthate	Hydrothermal method	>90	[78]
PANI/TiO$_2$/metakaolin	Visible light irradiation	Butyl xanthate	Sol–gel and in-situ polymerization	94.8	[79]
MoS$_2$/TiO$_2$/clinoptilolite	Visible light irradiation	Sodium isopropyl xanthate	Moderate hydrothermal route	>90	[80]
b-TiO$_2$ @MoS$_2$	Visible light irradiation	Butyl xanthate	Sol-gel method	94.80	[81]
TiO$_2$/ graphene nanocomposites	Visible light irradiation	Potassium butyl xanthate	Hydrothermal method	97.03	[15]
TiO$_2$/g-C$_3$N$_4$	Visible light irradiation	Potassium butyl xanthate	Hydrothermal method	97.10	[82]
C, N, S-tridoped TiO$_2$ nanotubes	Visible light irradiation	Potassium ethyl xanthate	Hydrothermal method	-	[83]
A-BiFe/Bent	Visible light irradiation	Ethyl xanthate	Mechanically activated	98.60	[84]
A-BiFe/Bent	Visible light irradiation	Ethyl xanthate	Mechanically activated	97.85	[85]
A-BiFe/Bent	Visible light irradiation	Ethyl xanthate	Mechanically activated	98.43	[86]
micro graphite/BiOI	Visible light irradiation	Xanthate	Hydrothermal	94.36	[51]
S-scheme BiOBr/g-C$_3$N$_4$	Visible light irradiation	Ethyl xanthate	Hydrothermal	96.10	[87]
(BiO)$_2$CO$_3$ nanowires	UV-visible light irradiation	Sodium isopropyl xanthate	Hydrothermal	96.00	[88]
Fe^{3+}-doped (BiO)$_2$CO$_3$	UV-visible light irradiation	Sodium isopropyl xanthate	Hydrothermal	95.71	[89]
BiOBr@TiO$_2$/PU-SF	Visible light irradiation	Ethyl xanthate	A facile blending-phase separation-impregnation-precipitation	97.85	[90]
BiOCl/TiO$_2$/clinoptilolite	Visible light irradiation	Sodium isopropyl xanthate	A facile hydrothermal route combining with a water bath precipitation procedure	>90	[91]
PW9@ZnO/Ag	UV-visible light irradiation	Butyl xanthate	Hydrothermal	99.83	[28]

Doping modification mainly involves the introduction of new elements into the TiO$_2$ crystal lattice, which leads to the generation of lattice defects in TiO$_2$ and then causes a change in the energy band structure. This can effectively inhibit the complexation of photogenerated electron-hole pairs and narrow the band gap energy. It also causes the generation of oxygen vacancies in TiO$_2$, resulting in the extension of the light absorption range, from the UV region to the visible region, and enhances the TiO$_2$ photocatalytic activity [92,93]. Doping modification mainly consists of metal ion doping, non-metal ion doping, and noble metal doping. Metal ion doping mainly utilizes Cu^{2+}, Mn^{2+}, and Fe^{3+} [94–96]. Non-metal ion doping primarily includes C, N, and S [97]. The doping of noble metals mostly involves Au and Ag [98].

Bian et al. [77] demonstrated that nitrogen-cerium co-doped TiO$_2$ showed an effective degradation of xanthate under visible light irradiation. This work synthesized new Ce/N-TiO$_2$@AC photocatalysts using the sol-gel method, which achieved 96.3% SIBX removal under visible light irradiation. This degradation process can be briefly described as follows:

the SIBX molecules were first adsorbed on the surface of the Ce/N-TiO$_2$@AC photocatalyst. Subsequently, the band gap of TiO$_2$ was significantly reduced. This suggested that the valence band (vB) of TiO$_2$ could be strongly activated to form holes (h$^+$), while photoinduced electrons (e$^-$) could be further activated into the conduction band (cB). In addition, the electrons captured in the Ce^{4+}/Ce^{3+} sites could be transferred to the catalyst surface, leading to the generation of numerous strong oxidation free radicals (e.g., $\bullet$O$_2^-$ and $\bullet$OH). Finally, the SIBX molecules attacked by these radicals could be completely decomposed into inorganic sulfates (SO$_4^{2-}$). Li et al. [14] evaluated the effects of Ag-TiO$_2$-FAMB photocatalysts on the photocatalytic degradation performance of butyl sodium xanthate. This work summarized the potential mechanisms of xanthate degradation, as shown in Figure 5. The results of free radical quenching tests showed that superoxide radicals ($\bullet$O$_2^-$), hydroxyl radicals ($\bullet$OH), and photogenerated holes (h$^+$) play a joint role in the photocatalytic degradation of sodium butyl xanthate. Among them, superoxide radicals ($\bullet$O$_2^-$) play a major role in the degradation of xanthate. Furthermore, the pathway of xanthate degradation showed that peroxanthate (C$_4$H$_9$OCSSO$^-$) was the intermediate product of the xanthate degradation process, and xanthate was finally degraded to CO$_2$, SO$_4^{2-}$, and H$_2$O.
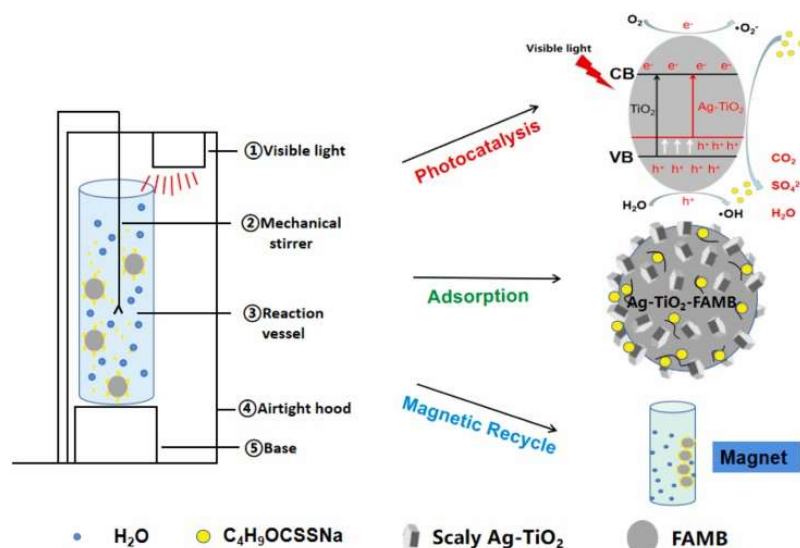
Figure 5. Xanthate degradation mechanism diagram (Reproduced from Colloids Surf. Physicochem. Eng. Aspects 2021, 624 with permission from Elsevier) [14].

Recent studies have shown that Ag/semiconductor/clay mineral terpolymer composites present excellent adsorption and photocatalytic synergistic effects for pollutant degradation [99]. Zeolite has a promising application as a TiO$_2$ carrier, due to its abundant porous structure and stable chemical properties [100]. Shen et al. [78] indicated that TiO$_2$/clinoptilolite showed an excellent performance for photodegradation of SIPX compared with that of pure TiO$_2$. The fast degradation of SIPX under UV irradiation was attributed to the synergistic effect of the clinoptilolite adsorbent and TiO$_2$ photocatalyst in the composite nanoparticles. The SIPX was eventually degraded to small molecule inorganic pollutants such as CO$_2$ and SO$_4^{2-}$. Zhou et al. [101] investigated the photocatalytic degradation mechanism on xanthate pollutants with Ag/TiO$_2$/clinoptilolite (ATC) nanocomposite as a composite catalyst. The results showed that the photogenerated electrons reacted with the absorbed O$_2$ to produce $\bullet$O$_2^-$, and the generation of holes on the TiO$_2$ valence band could react with OH$^-$ and H$_2$O to produce $\bullet$OH. Then, the $\bullet$O$_2^-$ and $\bullet$OH could oxidize xanthate directly to CO$_2$ and H$_2$O. Tan and co-workers reported that the new PANI/TiO$_2$/metakaolin showed desirable performance in the degradation of butyl xanthate with visible light irradiation compared to pure TiO$_2$ [79]. The excellent adsorption of butylxanthate of the composites facilitated the removal of xanthate within 4 h under visible light irradiation, and the degradation rate reached 94.8%.

Recently, two-dimensional nanomaterials have been used as co-catalysts, such as graphene oxide (GO), graphitic phase carbon nitride (g-C_3N_4), and molybdenum disulfide (MoS_2) to promote the photocatalytic activity of single TiO_2. These 2D nanomaterials have narrow band gaps and can be coupled with TiO_2 to form heterogeneous structures. Zhou et al. [80] prepared a new MoS_2/TiO_2/clinoptilolite (MTC) nanocomposite with ternary non-homogeneous, which showed an excellent photocatalytic activity under visible light irradiation. The excellent adsorption capacity of clinoptilolite and the MoS_2/TiO_2 heterostructures in the nanocomposites provided favorable conditions for the efficient degradation of xanthate. Tang et al. [81] prepared b-TiO_2@MoS_2 heterostructures using electrochemical exfoliation combined with a sol-gel technique. This heterostructure showed stronger visible light absorption and broader active sites than the pure b-TiO_2 material, and also facilitated the separation and transfer of photogenerated charges. Under visible light irradiation, the maximum efficiency of xanthate degradation could reach 94.80% at a catalyst loading of 0.03 g. New TiO_2/graphene (TiO_2/GO) composite photocatalytic materials were synthesized and used as photocatalysts to treat xanthate wastewater [15]. The degradation xanthate mechanism is shown in Figure 6. The electrons were transferred from the valence band to the conduction band to generate electron-hole pairs, promoting the formation of strong oxidation free radicals (e.g., $\bullet O_2^-$ and $\bullet OH$), and degraded the xanthate. Therefore, TiO_2/GO has great potential to treat xanthate wastewater, due to its huge specific surface area, smaller pore size, and lower electron–hole pair complexation rate.
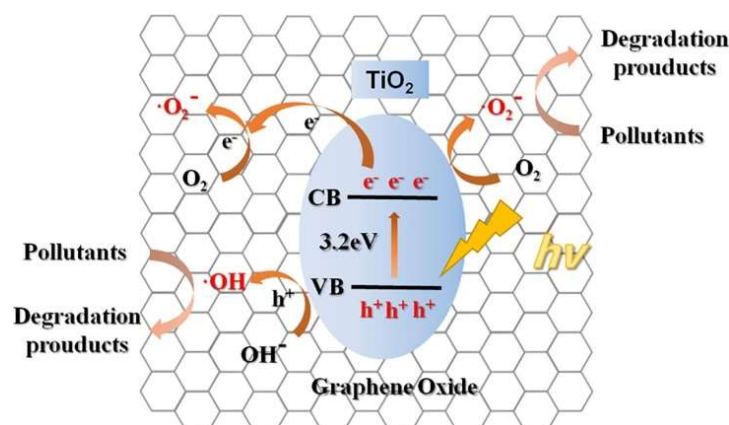
Figure 6. Mechanism of the degradation of xanthate (Reproduced from Chem. Eng. J. 2022, 431 with permission from Elsevier) [15].

Bi-Based Oxide Photocatalysts

Bismuth (Bi)-based oxide photocatalysts mainly include Bi_2O_3, bismuth oxide halide BiOX (X = Cl, Br, I), Bi_2MO (M = Cr, Mo, W), which have captured the attention of researches for application in flotation wastewater treatment, due to a high quantum yield, strong visible light response, and controllable structure [102,103]. The electronic structure of these bismuth-based materials is unique and exhibits a great photocatalytic degradation capacity under UV-vis irradiation [104]. However, the relatively small specific surface area and faster recombination of photogenerated carriers of single bismuth-based oxides lead to a less desirable photocatalytic activity for organic compounds [105]. Therefore, various strategies have been systematically investigated by researchers, such as heterojunctions, metal and non-metal doping, surface modification, and internal coupling between different bismuth metal oxides, to improve the photolytic ability of photocatalysts [106,107].

$BiFeO_3$ and $Bi_2Fe_4O_9$ as narrow band gap semiconductors have good magnetic properties, strong acid and alkali resistance, and excellent chemical stability, and are promising visible light drive materials [108,109]. Recently, Yang et al. prepared a bentonite-based bismuth ferrite composite containing $BiFeO_3$ and $Bi_2Fe_4O_9$ using a mechanical activation technique [84,85]. The activated bentonite-based bismuth ferrate (A-BiFe/Bent) was used as a non-homogeneous Fenton catalyst for the degradation of ethyl xanthate (EX) from

flotation wastewater. Excellent activity under visible light was observed, and the degradation pathway as well as a possible reaction mechanism for the catalytic degradation of EX were proposed, as shown in Figure 7 [84,85]. Similarly, as reported by Zhu et al. [83], A-BiFe/Bent as a catalyst combined with a persulfate (PS) activation system under visible light irradiation could effectively degrade ethylxanthate (EX), providing a potential pathway for the treatment of flotation wastewater.
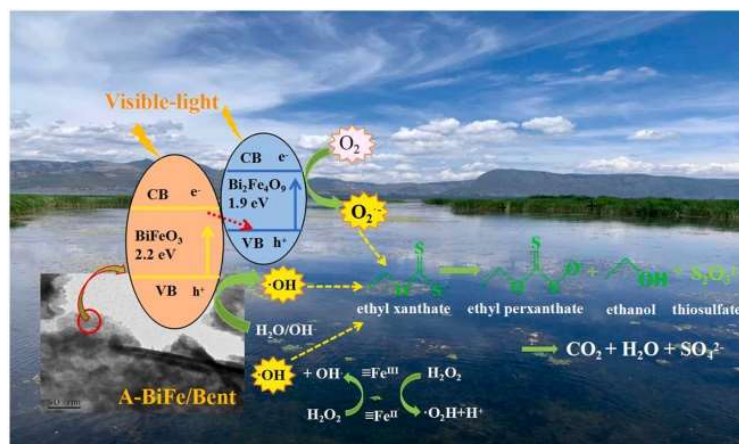

Figure 7. Mechanism of A-BiFe/Bent-catalyzed degradation of EX under visible light (reproduced from Opt. Mater. 2022, 132 with permission from Elsevier) [85].

In recent years, carbon-based materials such as graphite and 2D g-C_3N_4 have been widely used in the field of wastewater treatment, because of their large surface area and good adsorption properties [110]. Mic-g/BiOI nanocomposites showed superior photocatalytic activity in the removal of xanthate residues from sulfide ore flotation wastewater, with a 4.3-times higher removal rate than that of pure BiOI [86]. The reason for this was mainly attributed to the synergistic effect of the desirable contact interface between BiOI and graphite and the good electrical conductivity. Similarly, Yuan and co-workers [87] found that a BiOBr/g-$C_3N_4-10\%$ photocatalyst exhibited superior photodegradation activity of ethylxanthate in mineral flotation wastewater under visible light and had an excellent reusability compared with single BiOBr and g-C_3N_4. The increase in visible light-driven photodegradation activity was mainly attributed to the construction of S-scheme BiOBr/g-C_3N_4 heterojunctions and the effective separation of photogenerated carriers.

The application of alkaline bismuth subcarbonate (($BiO)_2CO_3$) as a novel photocatalyst has recently attracted considerable attention [88,111]. Cui et al. [88] obtained ($BiO)_2CO_3$ nanowire photocatalysts through a simple hydrothermal method and applied them to degrade sodium isopropylxanthate. It was shown that ($BiO)_2CO_3$ nanowires exhibited excellent photocatalytic degradation of xanthates, due to a narrow band gap under UV-vis irradiation. It was also found that ($BiO)_2CO_3@Bi_2S_3$ core-shell nanowires were produced during the photocatalytic decomposition of xanthate solution and showed an enhanced photocatalytic activity after repeated cycles of testing. However, the effect of the S content on the performance of core-shell ($BiO)_2CO_3@Bi_2S_3$ was still unclear. The luminescence (PL) properties of ($BiO)_2CO_3@Bi_2S_3$ core-shell nanowires with different S contents were further studied [111]. The results indicated that ($BiO)_2CO_3$ could be easily converted to Bi_2S_3 in the presence of S and rapidly formed ($BiO)_2CO_3@Bi_2S_3$ heterojunctions, which was beneficial for the efficient separation of electron-hole pairs. In addition, sodium isopropylxanthate was eventually oxidized to SO_4^{2-} and CO_2 by the ($BiO)_2CO_3$ nanowires doped with Fe^{3+} under UV light irradiation. The Fe^{3+}-doped ($BiO)_2CO_3$ nanowires exhibited excellent performance in the removal of sodium isopropylxanthate compared to pure ($BiO)_2CO_3$ nanowires, due to a narrow band gap and wider specific surface area [89].

ZnO-Based Photocatalysts

ZnO is an n-type semiconductor compound with high photosensitivity and thermal stability, which has the advantages of eco-friendliness, low band gap energy, and low cost. However, ZnO has a wide band gap of about 3.37 eV, resulting in easy recombination of the photogenerated carriers, and it only absorbs UV light <387 nm, which greatly limits its application in wastewater treatment [112,113]. To overcome these drawbacks, various modifications, such as elemental doping, and surface modification of noble metals and heterojunctions [114], have been applied to the ZnO structure, to extend its functionality under solar irradiation. In particular, element-doped nanocomposite photocatalysts have proven to be promising in the field of mine wastewater treatment.

ZnO doped with Mn and Fe was reported as an active photocatalyst for the production of oxygen from water under visible light irradiation. Xiao et al. [115,116] performed photocatalytic degradation of potassium ethylxanthate (KEX) under visible light irradiation with $Zn_{1-x}Mn_xO$ and $Zn_{1-x}Fe_xO$ photocatalysts. The results indicated that $Zn_{0.95}Mn_{0.05}O$ and $Zn_{0.96}Fe_{0.04}O$ presented excellent photocatalytic degradation efficiency for xanthate, due to the low complexation of photogenerated electron-hole pairs. Additionally, Xin and co-workers [28] synthesized new PW9@ZnO/Ag(PZA) composites that were doped with Ag nanoparticles using a hydrothermal method. The application of PZA to degrade BX in simulated wastewater under UV light and xenon lamp showed good photocatalytic degradation. Meanwhile, the mechanism of PZA photocatalysis was analyzed, including quantum photon absorption, electron-hole pair generation, and separation and redox reaction processes, as shown in Figure 8.
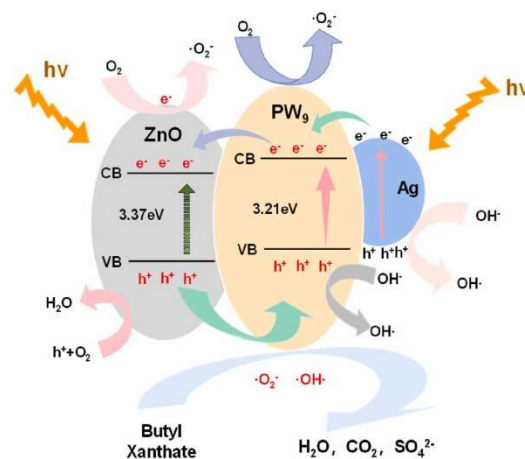

Figure 8. Diagram of the photocatalytic reaction mechanism (reproduced from Environ. Res. 2022, 214, 113776 with permission from Elsevier) [28].

4. Conclusions and Future Research Requirements for the Treatment of Xanthate Wastewater

The traditional coagulation–flocculation and adsorption methods usually have difficulty in making xanthate wastewater meet discharge standards, due to their relatively low removal rate. Biological methods fail to realize the clean degradation of xanthate fully, and the formation of CS_2 is toxic and still harmful to the environment. Thus, in the actual wastewater purification processes, a treatment method that can completely decompose the xanthate into small molecule compounds, such as CO_2, H_2O, and SO_4^{2-} would be the best candidate.

With the wide application of advanced oxidation processes (AOPs) in wastewater treatment, the Fenton and ozone oxidation have been extensively discussed in the field of xanthate wastewater treatment. This process utilizes the highly reactive ●OH that is generated by AOPs to oxidize and decompose the residual xanthate in wastewater. Due to the strong oxidizing ability of ●OH, this can make the organic substances of xanthate decompose rapidly and eventually mineralize into CO_2, H_2O, and SO_4^{2-}. Although the

research on catalytic oxidation technology has made great progress, there are still many problems that need to be solved. For example, the oxidative decomposition pathway and intermediate product analysis of xanthate in wastewater are still controversial. Furthermore, the complex and variable composition and nature of actual xanthate wastewaters render catalytic oxidation technology difficult to scale up for industrial applications.

Photocatalytic oxidation shows outstanding performance in the treatment of xanthate wastewater. The technique involves the generation of electron-hole pairs through electron transitions within the semiconductor under visible or ultraviolet light. This promotes the generation of highly reactive oxygen radicals, which further break down the xanthate molecule. However, various semiconductor photocatalysts have the disadvantages of a fast recombination of photogenerated electron-hole pairs and narrow light absorption range during the degradation of xanthate, so a great deal of research is still needed regarding improving the photocatalytic activity.

Briefly, the treatment of xanthate wastewater is of great significance for the sustainable development of the mineral processing industry and environmental protection. The available various treatment methods have both advantages and disadvantages. The main reasons being that the existing technology is quite specialized, focusing on a specific aspect. In other words, researchers have mainly studied the treatment of xanthate wastewater based on the perspective of single discipline, and this research paradigm is not conducive to technological innovation. Currently, the treatment effect, cost, and efficiency are usually not comprehensively assessed. Furthermore, most research is now focused on simulated xanthate wastewater at laboratory scale, while actual mine plant xanthate wastewater is less tested. In fact, actual mine plant xanthate wastewater often has more intricate physico-chemical properties. Thus, the adaptability and repeatability of each method needs to be highly valued, although desirable results can be obtained with simulated xanthate wastewater at laboratory scale. In addition, combined methods for the treatment of xanthate wastewater will be conducive to achieving high efficiency, low costs, and no secondary pollution. We believe that interdisciplinary research of a more organized manner may generate more original and innovative technologies for the treatment of xanthate wastewater in the future.

Author Contributions: Conceptualization, Writing-review and editing, J.Y.; Data curation, S.L.; Investigation, Data curation, Z.D.; Conceptualization, Methodology, J.L.; Visualization, Investigation, A.Y.; Conceptualization, Writing review and editing, S.B.; Supervision, S.W. All authors have read and agreed to the published version of the manuscript.

Data Availability Statement: The data presented in this study are available on request from the corresponding author.

Conflicts of Interest: The authors declare no conflict of interest.

References

1. Cheng, H.; Lin, H.; Huo, H.; Dong, Y.; Xue, Q.; Cao, L. Continuous removal of ore floatation reagents by an anaerobic-aerobic biological filter. *Bioresour. Technol.* **2012**, *114*, 255–261. [CrossRef] [PubMed]
2. Pearse, M.J. An overview of the use of chemical reagents in mineral processing. *Miner. Eng.* **2005**, *18*, 139–149. [CrossRef]
3. Amrollahi, A.; Massinaei, M.; Zeraatkar Moghaddam, A. Removal of the residual xanthate from flotation plant tailings using bentonite modified by magnetic nano-particles. *Miner. Eng.* **2019**, *134*, 142–155. [CrossRef]
4. Natarajan, K.A.; Prakasan, M.R.S. Biodegradation of sodium isopropyl xanthate by paenibacillus polymyxa and pseudomonas putida. *Miner. Metall. Process.* **2013**, *30*, 226–232. [CrossRef]
5. Zhang, X.; Zhao, Y.; Zhang, Z.; Wang, S. Investigation of the interaction between xanthate and kaolinite based on experiments, molecular dynamics simulation, and density functional theory. *J. Mol. Liq.* **2021**, *336*, 116298. [CrossRef]
6. García-Leiva, B.; Teixeira, L.A.C.; Torem, M.L. Degradation of xanthate in waters by hydrogen peroxide, fenton and simulated solar photo-fenton processes. *J. Mater. Res. Technol.* **2019**, *8*, 5698–5706. [CrossRef]
7. Wang, L.; Fu, P.; Ma, Y.; Zhang, X.; Zhang, Y.; Yang, X. Steel slag as a cost-effective adsorbent for synergic removal of collectors, Cu(II) and Pb(II) ions from flotation wastewaters. *Miner. Eng.* **2022**, *183*, 107593. [CrossRef]

8. Sun, Z.X.; Forsling, W. The degradation kinetics of ethyl-xanthate as a function of pH in aqueous solution. *Miner. Eng.* **1997**, *10*, 389–400. [CrossRef]

9. Behnamfard, A.; Veglio, F. Estimation of xanthate decomposition percentage as a function of pH, temperature and time by least squares regression and adaptive neuro-fuzzy inference system. *Int. J. Min. Geo-Eng.* **2019**, *53*, 157–163.

10. Yang, C.; Gao, P.; Dang, M.; Liu, Y.; Yao, F.; Ge, L.; Guo, L.; Tao, Y. Research progress on treatment process of xanthate in beneficiation wastewater. *J. Xuzhou Inst. Technol.* **2022**, *37*, 62–70+92. (In Chinese) [CrossRef]

11. Rezaei, R.; Massinaei, M.; Zeraatkar Moghaddam, A. Removal of the residual xanthate from flotation plant tailings using modified bentonite. *Miner. Eng.* **2018**, *119*, 1–10. [CrossRef]

12. Mielczarski, J. The role of impurities of sphalerite in the adsorption of ethyl xanthate and its flotation. *Int. J. Miner. Process.* **1986**, *16*, 179–194. [CrossRef]

13. Dong, Y.B.; Lin, H.; Liu, Q.L.; Huo, H.X. Treatment of flotation wastewater using biological activated carbon. *J. Cent. South Univ.* **2014**, *21*, 3580–3587. [CrossRef]

14. Li, G.; Teng, Q.; Sun, B.; Yang, Z.; Liu, S.; Zhu, X. Synthesis scaly Ag-TiO$_2$ loaded fly ash magnetic bead particles for treatment of xanthate wastewater. *Colloids Surf. Physicochem. Eng. Asp.* **2021**, *624*, 126795. [CrossRef]

15. Jiang, M.; Zhang, M.; Wang, L.; Fei, Y.; Wang, S.; Núñez-Delgado, A.; Bokhari, A.; Race, M.; Khataee, A.; Jaromír Klemeš, J.; et al. Photocatalytic degradation of xanthate in flotation plant tailings by TiO$_2$/graphene nanocomposites. *Chem. Eng. J.* **2022**, *431*, 134104. [CrossRef]

16. Fu, P.; Feng, J.; Yang, H.; Yang, T. Degradation of sodium n-butyl xanthate by vacuum UV-ozone (VUV/O$_3$) in comparison with ozone and VUV photolysis. *Process Saf. Environ. Prot.* **2016**, *102*, 64–70. [CrossRef]

17. Chen, S.H.; Du, D.Y. Degradation of n-butyl xanthate using fly ash as heterogeneous Fenton-like catalyst. *J. Cent. South Univ.* **2014**, *21*, 1448–1452. [CrossRef]

18. Martins, T.A.G.; Falconi, I.B.A.; Pavoski, G.; de Moraes, V.T.; Galluzzi Baltazar, M.d.P.; Espinosa, D.C.R. Green synthesis, characterization, and application of copper nanoparticles obtained from printed circuit boards to degrade mining surfactant by Fenton process. *J. Environ.* **2021**, *9*, 106576. [CrossRef]

19. Ai, G.H.; Tao, X.X.; Wang, Y.; Chen, Y.L. Removal of Xanthate in Flotation Wastewater by Ultrasound and Fenton Reagent. *Int. Conf. Electr. Technol. Civ. Eng.* **2011**, 6106–6110.

20. Chen, X.H.; Hu, Y.H.; Peng, H.; Cao, X.F. Degradation of ethyl xanthate in flotation residues by hydrogen peroxide. *J. Cent. South Univ.* **2015**, *22*, 495–501. [CrossRef]

21. Elizondo-Álvarez, M.A.; Uribe-Salas, A.; Bello-Teodoro, S. Chemical stability of xanthates, dithiophosphinates and hydroxamic acids in aqueous solutions and their environmental implications. *Ecotoxicol. Environ. Saf.* **2021**, *207*, 111509. [CrossRef] [PubMed]

22. Bararunyeretse, P.; Yao, J.; Dai, Y.; Bigawa, S.; Guo, Z.; Zhu, M. Toxic effect of two kinds of mineral collectors on soil microbial richness and activity: Analysis by microcalorimetry, microbial count, and enzyme activity assay. *Environ. Sci. Pollut. Res. Int.* **2017**, *24*, 1565–1577. [CrossRef]

23. Li, N.; Chen, Y.; Zhang, C.; Zhou, W.; Fu, M.Y.; Chen, W.L.; Wang, S. Highly Sensitive Determination of Butyl Xanthate in Surface and Drinking Water by Headspace Gas Chromatography with Electron Capture Detector. *Chromatographia* **2015**, *78*, 1305–1310. [CrossRef]

24. Mosevich, M.V.; Arshanitsa, N.M.; Glukhova, L.V. Substantiation of the maximum Permissible concentration of bytul sodium xanthate for fishery water bodies. *Chem. Abstr.* **1977**, *87*, 266.

25. Li, H.; Yao, J.; Duran, R.; Liu, J.; Min, N.; Chen, Z.; Zhu, X.; Zhao, C.; Ma, B.; Pang, W.; et al. Toxic response of the freshwater green algae Chlorella pyrenoidosa to combined effect of flotation reagent butyl xanthate and nickel. *Environ. Pollut.* **2021**, *286*, 117285. [CrossRef] [PubMed]

26. Liu, R.; Sun, W.; Ouyang, K.; Zhang, L.; Hu, Y. Decomposition of sodium butyl xanthate (SBX) in aqueous solution by means of OCF: Ozonator combined with flotator. *Miner. Eng.* **2015**, *70*, 222–227. [CrossRef]

27. Lou, J.; Lu, G.; Wei, Y.; Zhang, Y.; An, J.; Jia, M.; Li, M. Enhanced degradation of residual potassium ethyl xanthate in mineral separation wastewater by dielectric barrier discharge plasma and peroxymonosulfate. *Sep. Purif. Technol.* **2022**, *282*, 119955. [CrossRef]

28. Xin, Z.; Wang, S.; He, Q.; Han, X.; Fu, Z.; Xu, X.; Zhao, X. Preparation of a novel photocatalytic catalyst PW9@ZnO/Ag and the photocatalytic degradation of butyl xanthate under visible light. *Environ. Res.* **2022**, *214*, 113776. [CrossRef]

29. Yanev, S.G.; Kent, U.M.; Roberts, E.S.; Ballou, D.P.; Hollenberg, P.F. Mechanistic studies of cytochrome P450 2B1 inactivation by xanthates. *Arch. Biochem. Biophys.* **2000**, *378*, 157–166. [CrossRef]

30. Yang, Y.; Li, Y.; Zhang, Y.M.; Liang, D.W. Applying hybrid coagulants and polyacrylamide flocculants in the treatment of high-phosphorus hematite flotation wastewater (HHFW): Optimization through response surface methodology. *Sep. Purif. Technol.* **2010**, *76*, 72–78. [CrossRef]

31. Meng, X.; Wu, J.; Kang, J.; Gao, J.; Liu, R.; Gao, Y.; Wang, R.; Fan, R.; Khoso, S.A.; Sun, W.; et al. Comparison of the reduction of chemical oxygen demand in wastewater from mineral processing using the coagulation–flocculation, adsorption and Fenton processes. *Miner. Eng.* **2018**, *128*, 275–283. [CrossRef]

32. Xia, C.; Luo, Y.; Yao, J.; Liu, W.; Wang, F.; Wu, X. Joint effects of Cd and thioglycollic acid on soil microbial activity. *Int. Biodeterior. Biodegrad.* **2018**, *128*, 164–170. [CrossRef]

33.　Sun, W.; Huang, H.; Cao, X.F.; Meng, W.; Dong, D. Study on the Treating Methods of High Concentration Organic Wastewater in Production of Xanthate. *Nonferr. Met.* **2012**, *2*, 47–50. (In Chinese) [CrossRef]

34.　Salarirad, M.M.; Behnamfard, A.; Veglio, F. Removal of xanthate from aqueous solutions by adsorption onto untreated and acid/base treated activated carbons. *Desalin. Water Treat.* **2021**, *212*, 220–233. [CrossRef]

35.　Huang, Q.; Li, X.; Ren, S.; Luo, W. Removal of ethyl, isobutyl, and isoamyl xanthates using cationic gemini surfactant-modified montmorillonites. *Colloids Surf. Physicochem. Eng. Asp.* **2019**, *580*, 123723. [CrossRef]

36.　Oliveira, C.R.; Rubio, J. Isopropylxanthate ions uptake by modified natural zeolite and removal by dissolved air flotation. *Int. J. Miner. Process.* **2009**, *90*, 21–26. [CrossRef]

37.　Li, L.; He, M.; Feng, Y.; Wei, H.; You, X.; Yu, H.; Wang, Q.; Wang, J. Adsorption of xanthate from aqueous solution by multilayer graphene oxide: An experimental and molecular dynamics simulation study. *Adv. Compos. Hybrid Mater.* **2021**, *4*, 725–732. [CrossRef]

38.　Chen, S.; Gong, W.; Mei, G. Experimental Study on the Biodegradability of Alkyl Xanthate Collectors. *Acta Sci. Nat. Univ. Pekinensis.* **2010**, *46*, 351–357. (In Chinese) [CrossRef]

39.　Zeng, Y.; Tang, L.; Zhang, M. Progress research on the treatment technology of residual xanthate in mineral concentration wastewater and its mechanism. *Ind. Water Treat.* **2010**, *30*, 8–10+49. (In Chinese)

40.　Chen, S.; Gong, W.; Mei, G.; Zhou, Q.; Bai, C.; Xu, N. Primary biodegradation of sulfide mineral flotation collectors. *Miner. Eng.* **2011**, *24*, 953–955. [CrossRef]

41.　Lin, H.; Qin, K.; Dong, Y.; Li, B. A newly-constructed bifunctional bacterial consortium for removing butyl xanthate and cadmium simultaneously from mineral processing wastewater: Experimental evaluation, degradation and biomineralization. *J. Environ. Manag.* **2022**, *316*, 115304. [CrossRef] [PubMed]

42.　Chockalingam, E.; Subramanian, S.; Natarajan, K.A. Studies on biodegradation of organic flotation collectors using Bacillus polymyxa. *Hydrometallurgy* **2003**, *71*, 249–256. [CrossRef]

43.　Molina, G.C.; Cayo, C.H.; Rodrigues, M.A.S.; Bernardes, A.M. Sodium isopropyl xanthate degradation by advanced oxidation processes. *Miner. Eng.* **2013**, *45*, 88–93. [CrossRef]

44.　Li, S.; Wu, Y.; Zheng, H.; Li, H.; Zheng, Y.; Nan, J.; Ma, J.; Nagarajan, D.; Chang, J.S. Antibiotics degradation by advanced oxidation process (AOPs): Recent advances in ecotoxity and antibiotic-resistance genes induction of degradation products. *Chemosphere* **2022**, *311*, 136977. [CrossRef]

45.　Dong, C.; Fang, W.; Yi, Q.; Zhang, J. A comprehensive review on reactive oxygen species (ROS) in advanced oxidation processes (AOPs). *Chemosphere* **2022**, *308*, 136205. [CrossRef]

46.　Lin, R.; Li, Y.; Yong, T.; Cao, W.; Wu, J.; Shen, Y. Synergistic effects of oxidation, coagulation and adsorption in the integrated fenton-based process for wastewater treatment: A review. *J. Environ. Manag.* **2022**, *306*, 114460. [CrossRef] [PubMed]

47.　Zhang, M.H.; Dong, H.; Zhao, L.; Wang, D.X.; Meng, D. A review on Fenton process for organic wastewater treatment based on optimization perspective. *Sci. Total Environ.* **2019**, *670*, 110–121. [CrossRef] [PubMed]

48.　Yuan, J.; Ding, Z.; Bi, Y.; Li, J.; Wen, S.; Bai, S. Resource Utilization of Acid Mine Drainage (AMD): A Review. *Water.* **2022**, *14*, 2385. [CrossRef]

49.　Bello, M.M.; Abdul Raman, A.A.; Asghar, A. A review on approaches for addressing the limitations of Fenton oxidation for recalcitrant wastewater treatment. *Process Saf. Environ. Prot.* **2019**, *126*, 119–140. [CrossRef]

50.　Ai, G.H.; Tu, Y.Q. Degradation of Residual Xanthate of in Sulfide Mineral Processing Wastewater by Fenton Reagent. *Int. Conf. Electr. Technol. Civ. Eng.* **2011**, 3046–3049.

51.　Zheng, Y.; Yuan, F.; Gao, D.; Liu, L.; Wang, L.; Hu, X. Improved visible-light-driven activity of micro graphite/BiOI nanocomposite for effective removal of xanthate from wastewater. *Mater. Res. Bull.* **2023**, *158*, 112080. [CrossRef]

52.　Wei, G.; Li, Y.; Cai, S.; Li, Z.; Mo, J.; Zhang, L. Photo-Fenton degradation of ethyl xanthate catalyzed by bentonite-supported Fe(II)/phosphotungstic acid under visible light irradiation. *Water Sci. Technol.* **2018**, *2017*, 473–480. [CrossRef] [PubMed]

53.　Shokri, A.; Fard, M.S. A critical review in Fenton-like approach for the removal of pollutants in the aqueous environment. *Environ. Chall.* **2022**, *7*, 100534. [CrossRef]

54.　Wang, N.; Zheng, T.; Zhang, G.; Wang, P. A review on Fenton-like processes for organic wastewater treatment. *J. Environ. Chem. Eng.* **2016**, *4*, 762–787. [CrossRef]

55.　Shao, L.; Wei, G.; Wang, Y.; Li, Z.; Zhang, L.; Zhao, S.; Zhou, M. Preparation and application of acidified/calcined red mud catalyst for catalytic degradation of butyl xanthate in Fenton-like process. *Environ. Sci. Pollut. Res. Int.* **2016**, *23*, 15202–15207. [CrossRef]

56.　Rekhate, C.V.; Srivastava, J.K. Recent advances in ozone-based advanced oxidation processes for treatment of wastewater—A review. *Adv. Chem. Eng.* **2020**, *3*, 100031. [CrossRef]

57.　Umar, M.; Roddick, F.; Fan, L.; Aziz, H.A. Application of ozone for the removal of bisphenol A from water and wastewater—A review. *Chemosphere* **2013**, *90*, 2197–2207. [CrossRef]

58.　Wang, J.; Bai, Z. Fe-based catalysts for heterogeneous catalytic ozonation of emerging contaminants in water and wastewater. *Chem. Eng. J.* **2017**, *312*, 79–98. [CrossRef]

59.　Wang, J.; Chen, H. Catalytic ozonation for water and wastewater treatment: Recent advances and perspective. *Sci. Total Environ.* **2020**, *704*, 135249. [CrossRef]

60. Zhang, M.; Liu, J.S. Study on degradation of flotation reagents butyl xanthate by zone. *Chin. J. Environ. Eng.* **2011**, *5*, 2712–2716. (In Chinese)

61. Kiyanmehr, K.; Moussavi, G.; Mohammadi, S.; Naddafi, K.; Giannakis, S. The efficacy of the VUV/O_3 process run in a continuous-flow fluidized bed reactor for simultaneous elimination of favipiravir and bacteria in aqueous matrices. *Chemosphere* **2022**, *304*, 135307. [CrossRef] [PubMed]

62. Fu, P.; Feng, J.; Yang, T.; Yang, H. Comparison of alkyl xanthates degradation in aqueous solution by the O_3 and UV/O_3 processes: Efficiency, mineralization and ozone utilization. *Miner. Eng.* **2015**, *81*, 128–134. [CrossRef]

63. Fu, P.; Wang, L.; Ma, Y.; Hou, Z. A comparative study on the degradation of ethyl xanthate collector by O_3, UV254nm, UV185+254nm, O3/UV254nm and O3/UV185+254nm processes. *J. Environ. Chem. Eng.* **2020**, *8*. [CrossRef]

64. Yan, P.; Chen, G.; Ye, M.; Sun, S.; Ma, H.; Lin, W. Oxidation of potassium n -butyl xanthate with ozone: Products and pathways. *J. Clean. Prod.* **2016**, *139*, 287–294. [CrossRef]

65. Koelsch, M.; Cassaignon, S.; Ta Thanh Minh, C.; Guillemoles, J.F.; Jolivet, J.P. Electrochemical comparative study of titania (anatase, brookite and rutile) nanoparticles synthesized in aqueous medium. *Thin Solid Films* **2004**, *451–452*, 86–92. [CrossRef]

66. Etacheri, V.; Di Valentin, C.; Schneider, J.; Bahnemann, D.; Pillai, S.C. Visible-light activation of TiO_2 photocatalysts: Advances in theory and experiments. *J. Photochem. Photobiol. C.* **2015**, *25*, 1–29. [CrossRef]

67. Banerjee, S.; Pillai, S.C.; Falaras, P.; O'Shea, K.E.; Byrne, J.A.; Dionysiou, D.D. New Insights into the Mechanism of Visible Light Photocatalysis. *J. Phys. Chem. Lett.* **2014**, *5*, 2543–2554. [CrossRef]

68. Lim, T.-T.; Yap, P.-S.; Srinivasan, M.; Fane, A.G. TiO_2/AC Composites for Synergistic Adsorption-Photocatalysis Processes: Present Challenges and Further Developments for Water Treatment and Reclamation. *Crit. Rev. Environ. Sci. Technol.* **2011**, *41*, 1173–1230. [CrossRef]

69. Litter, M.I. Heterogeneous photocatalysis Transition metal ions in photocatalytic systems. *Appl. Catal. B* **1999**, *23*, 89–144. [CrossRef]

70. Banerjee, S.; Dionysiou, D.D.; Pillai, S.C. Self-cleaning applications of TiO_2 by photo-induced hydrophilicity and photocatalysis. *Appl. Catal. B.* **2015**, *176–177*, 396–428. [CrossRef]

71. Zhou, W.; Yin, Z.; Du, Y.; Huang, X.; Zeng, Z.; Fan, Z.; Liu, H.; Wang, J.; Zhang, H. Synthesis of few-layer MoS_2 nanosheet-coated TiO_2 nanobelt heterostructures for enhanced photocatalytic activities. *Small* **2013**, *9*, 140–147. [CrossRef]

72. Su, J.; Yu, S.; Xu, M.; Guo, Y.; Sun, X.; Fan, Y.; Zhang, Z.; Yan, J.; Zhao, W. Enhanced visible light photocatalytic performances of few-layer $MoS_2@TiO_2$ hollow spheres heterostructures. *Mater. Res. Bull.* **2020**, *130*, 110936. [CrossRef]

73. Zhang, W.; Xiao, X.; Zheng, L.; Wan, C. Fabrication of $TiO_2/MoS_2@zeolite$ photocatalyst and its photocatalytic activity for degradation of methyl orange under visible light. *Appl. Surf. Sci.* **2015**, *358*, 468–478. [CrossRef]

74. Gao, H.; Zhang, P.; Hu, J.; Pan, J.; Fan, J.; Shao, G. One-dimensional Z-scheme $TiO_2/WO_3/Pt$ heterostructures for enhanced hydrogen generation. *Appl. Surf. Sci.* **2017**, *391*, 211–217. [CrossRef]

75. Asahi, R.; Morikawa, T.; Ohwaki, T.; Aoki, K.; Taga, Y. Visible-light photocatalysis in nitrogen-doped titanium oxides. *Science* **2001**, *293*, 269–271. [CrossRef] [PubMed]

76. Ghosh, S.; Kouamé, N.A.; Ramos, L.; Remita, S.; Dazzi, A.; Deniset-Besseau, A.; Beaunier, P.; Goubard, F.; Aubert, P.H.; Remita, H. Conducting polymer nanostructures for photocatalysis under visible light. *Nat. Mater.* **2015**, *14*, 505–511. [CrossRef]

77. Bian, Z.; Feng, Y.; Li, H.; Yu, H.; Wu, H. Adsorption-photocatalytic degradation and kinetic of sodium isobutyl xanthate using the nitrogen and cerium co-doping TiO_2-coated activated carbon. *Chemosphere* **2021**, *263*, 128254. [CrossRef]

78. Shen, Y.; Zhou, P.; Zhao, S.; Li, A.; Chen, Y.; Bai, J.; Han, C.; Wei, D.; Ao, Y. Synthesis of high-efficient $TiO_2/clinoptilolite$ photocatalyst for complete degradation of xanthate. *Miner. Eng.* **2020**, *159*, 106640. [CrossRef]

79. Tan, Y.; Chen, T.; Zheng, S.; Sun, Z.; Li, C. Adsorptive and photocatalytic behaviour of $PANI/TiO_2/metakaolin$ composites for the removal of xanthate from aqueous solution. *Miner. Eng.* **2021**, *171*, 107129. [CrossRef]

80. Zhou, P.; Shen, Y.; Zhao, S.; Chen, Y.; Gao, S.; Liu, W.; Wei, D. Hydrothermal synthesis of novel ternary hierarchical $MoS_2/TiO_2/clinoptilolite$ nanocomposites with remarkably enhanced visible light response towards xanthates. *Appl. Surf. Sci.* **2021**, *542*, 148578. [CrossRef]

81. Tang, Z.; Xu, L.; Shu, K.; Yang, J.; Tang, H. Fabrication of $TiO_2 @MoS_2$ heterostructures with improved visible light photocatalytic activity. *Colloids Surf. Physicochem. Eng. Asp.* **2022**, *642*, 128686. [CrossRef]

82. Zhang, M.; Han, N.; Fei, Y.; Liu, J.; Xing, L.; Núñez-Delgado, A.; Jiang, M.; Liu, S. $TiO_2/g-C_3N_4$ photocatalyst for the purification of potassium butyl xanthate in mineral processing wastewater. *J. Environ. Manag.* **2021**, *297*, 113311. [CrossRef] [PubMed]

83. Xiao, Q.; Ouyang, L. Photocatalytic photodegradation of xanthate over C, N, S-tridoped TiO_2 nanotubes under visible light irradiation. *J. Phys. Chem. Solids* **2011**, *72*, 39–44. [CrossRef]

84. Zhu, Y.; Wei, G.; Duan, G.; Yang, Y.; Zhang, L.; Li, Z.; Pei, R.; Luo, D. Heterogeneous activation of persulfate by mechanically activated bentonite-based bismuth ferrite composites under visible light for ethyl xanthate degradation: Application performance and catalytic mechanism. *Opt. Mater.* **2022**, *125*, 112089. [CrossRef]

85. Yang, Y.; Zhang, L.; Zhu, Y.; Wei, G.; Li, Z.; Mo, R. Three-dimensional photoelectrocatalytic degradation of ethyl xanthate catalyzed by activated bentonite-based bismuth ferrites particle electrodes: Influencing factors, kinetics, and mechanism. *J. Environ. Chem. Eng.* **2021**, *9*, 105559. [CrossRef]

86. Yang, Y.; Wei, G.; Zhu, Y.; Zhang, L.; Li, Z.; Li, Z.; Ding, X. Mechanism study of ethyl xanthate degradation catalyzed by activated bentonite-based bismuth ferrites composite in visible-light-driven photo-Fenton process. *Opt. Mater.* **2022**, *132*, 112855. [CrossRef]

87. Yuan, F.; Zheng, Y.; Gao, D.; Wang, L.; Hu, X. Facile assembly and enhanced visible-light-driven photocatalytic activity of S-scheme BiOBr/g-C_3N_4 heterojunction for degrading xanthate in wastewater. *J. Mol. Liq.* **2022**, *366*, 120279. [CrossRef]

88. Cui, K.; He, Y.; Jin, S. Enhanced UV-visible response of bismuth subcarbonate nanowires for degradation of xanthate and photocatalytic reaction mechanism. *Chemosphere* **2016**, *149*, 245–253. [CrossRef]

89. Guo, Y.; Cui, K.; Hu, M.; Jin, S. Fe(III) ions enhanced catalytic properties of $(BiO)_2CO_3$ nanowires and mechanism study for complete degradation of xanthate. *Chemosphere* **2017**, *181*, 190–196. [CrossRef]

90. Zou, M.; Tan, C.; Yang, H.; Kuang, D.; Nie, Z.; Zhou, H. Facile preparation of recyclable and flexible BiOBr@TiO_2/PU-SF composite porous membrane for efficient photocatalytic degradation of mineral flotation wastewater. *J. Water Process. Eng.* **2022**, *50*, 103127. [CrossRef]

91. Zhou, P.; Shen, Y.; Zhao, S.; Li, G.; Cui, B.; Wei, D.; Shen, Y. Synthesis of clinoptilolite-supported BiOCl/TiO_2 heterojunction nanocomposites with highly-enhanced photocatalytic activity for the complete degradation of xanthates under visible light. *Chem. Eng. J.* **2021**, *407*, 126697. [CrossRef]

92. Arora, I.; Chawla, H.; Chandra, A.; Sagadevan, S.; Garg, S. Advances in the strategies for enhancing the photocatalytic activity of TiO_2: Conversion from UV-light active to visible-light active photocatalyst. *Inorg. Chem. Commun.* **2022**, *143*, 109700. [CrossRef]

93. Serpone, N. Is the Band Gap of Pristine TiO_2 Narrowed by Anion- and Cation-Doping of Titanium Dioxide in Second-Generation Photocatalysts? *J. Phys. Chem. B* **2006**, *110*, 24287–24293. [CrossRef]

94. Guo, M.; Du, J. First-principles study of electronic structures and optical properties of Cu, Ag, and Au-doped anatase TiO_2. *Phys. B Condens. Matter* **2012**, *407*, 1003–1007. [CrossRef]

95. Ismael, M. Enhanced photocatalytic hydrogen production and degradation of organic pollutants from Fe (III) doped TiO_2 nanoparticles. *J. Environ. Chem. Eng.* **2020**, *8*, 103676. [CrossRef]

96. Latif, S.; Tahir, K.; Ullah Khan, A.; Abdulaziz, F.; Arooj, A.; Alanazi, T.Y.A.; Rakic, V.; Khan, A.; Jevtovic, V. Green synthesis of Mn-doped TiO_2 nanoparticles and investigating the influence of dopant concentration on the photocatalytic activity. *Inorg. Chem. Commun.* **2022**, *146*, 110091. [CrossRef]

97. Alkorbi, A.S.; Muhammad Asif Javed, H.; Hussain, S.; Latif, S.; Mahr, M.S.; Mustafa, M.S.; Alsaiari, R.; Alhemiary, N.A. Solar light-driven photocatalytic degradation of methyl blue by carbon-doped TiO_2 nanoparticles. *Opt. Mater.* **2022**, *127*, 112259. [CrossRef]

98. Khairy, M.; Kamar, E.M.; Mousa, M.A. Photocatalytic activity of nano-sized Ag and Au metal-doped TiO_2 embedded in rGO under visible light irradiation. *Mater. Sci. Eng.* **2022**, *286*, 116023. [CrossRef]

99. Liu, R.; Ji, Z.; Wang, J.; Zhang, J. Solvothermal synthesized Ag-decorated TiO_2/sepiolite composite with enhanced UV–vis and visible light photocatalytic activity. *Microporous Mesoporous Mater.* **2018**, *266*, 268–275. [CrossRef]

100. Ullah, R.; Liu, C.; Panezai, H.; Gul, A.; Sun, J.; Wu, X. Controlled crystal phase and particle size of loaded-TiO_2 using clinoptilolite as support via hydrothermal method for degradation of crystal violet dye in aqueous solution. *Arab. J. Chem.* **2020**, *13*, 4092–4101. [CrossRef]

101. Zhou, P.; Shen, Y.; Zhao, S.; Bai, J.; Han, C.; Liu, W.; Wei, D. Facile synthesis of clinoptilolite-supported Ag/TiO_2 nanocomposites for visible-light degradation of xanthates. *J. Taiwan Inst. Chem. Eng.* **2021**, *122*, 231–240. [CrossRef]

102. Ma, C.; Wei, J.; Jiang, K.; Chen, J.; Yang, Z.; Yang, X.; Yu, G.; Zhang, C.; Li, X. Typical layered structure bismuth-based photocatalysts for photocatalytic nitrogen oxides oxidation. *Sci. Total Environ.* **2023**, *855*, 158644. [CrossRef]

103. Guan, Y.; Liu, Y.; Lv, Q.; Wu, J. Bismuth-based photocatalyst for photocatalytic oxidation of flue gas mercury removal: A review. *J. Hazard. Mater.* **2021**, *418*, 126280. [CrossRef] [PubMed]

104. He, R.; Xu, D.; Cheng, B.; Yu, J.; Ho, W. Review on nanoscale Bi-based photocatalysts. *Nanoscale Horiz.* **2018**, *3*, 464–504. [CrossRef] [PubMed]

105. Zhu, Z.; Wan, S.; Zhao, Y.; Gu, Y.; Wang, Y.; Qin, Y.; Zhang, Z.; Ge, X.; Zhong, Q.; Bu, Y. Recent advances in bismuth-based multimetal oxide photocatalysts for hydrogen production from water splitting: Competitiveness, challenges, and future perspectives. *Mater. Rep. Energy* **2021**, *1*, 100019. [CrossRef]

106. Chawla, H.; Chandra, A.; Ingole, P.P.; Garg, S. Recent advancements in enhancement of photocatalytic activity using bismuth-based metal oxides Bi_2MO_6 (M = W, Mo, Cr) for environmental remediation and clean energy production. *J. Ind. Eng. Chem.* **2021**, *95*, 1–15. [CrossRef]

107. Li, H.; Li, J.; Ai, Z.; Jia, F.; Zhang, L. Oxygen Vacancy-Mediated Photocatalysis of BiOCl: Reactivity, Selectivity, and Perspectives. *Angew. Chem. Int. Ed. Engl.* **2018**, *57*, 122–138. [CrossRef]

108. Li, Z.; Dai, J.; Cheng, C.; Feng, W.; Wang, Q. Tailoring photocatalytic activity and magnetic properties of $BiFeO_3$/CeO_2/$Bi_2Fe_4O_9$ composites. *J. Phys. Chem. Solids* **2021**, *156*, 110171. [CrossRef]

109. Zhang, H.; Cheng, S.; Li, B.; Cheng, X.; Cheng, Q. Fabrication of magnetic Co/$BiFeO_3$ composite and its advanced treatment of pharmaceutical waste water by activation of peroxysulphate. *Sep. Purif. Technol.* **2018**, *202*, 242–247. [CrossRef]

110. Lu, S.; Shen, L.; Li, X.; Yu, B.; Ding, J.; Gao, P.; Zhang, H. Advances in the photocatalytic reduction functions of graphitic carbon nitride-based photocatalysts in environmental applications: A review. *J. Clean. Prod.* **2022**, *378*, 134589. [CrossRef]

111. Cui, K.; He, Y.; Jin, S.; Qian, H. Preparation, characterization, and photoluminescence property of core-shell $(BiO)_2CO_3$@Bi_2S_3 nanowires. *Mater. Chem. Phys.* **2018**, *211*, 65–71. [CrossRef]

112. Raza, W.; Faisal, S.M.; Owais, M.; Bahnemann, D.; Muneer, M. Facile fabrication of highly efficient modified ZnO photocatalyst with enhanced photocatalytic, antibacterial and anticancer activity. *RSC Adv.* **2016**, *6*, 78335–78350. [CrossRef]

113. Poongodi, G.; Anandan, P.; Kumar, R.M.; Jayavel, R. Studies on visible light photocatalytic and antibacterial activities of nanostructured cobalt doped ZnO thin films prepared by sol-gel spin coating method. *Spectrochim. Acta A Mol. Biomol.* **2015**, *148*, 237–243. [CrossRef] [PubMed]
114. Goktas, S.; Goktas, A. A comparative study on recent progress in efficient ZnO based nanocomposite and heterojunction photocatalysts: A review. *J. Alloys Compd.* **2021**, *863*, 158734. [CrossRef]
115. Xiao, Q.; Ouyang, L. Photocatalytic photodegradation of xanthate over Zn1−xMnxO under visible light irradiation. *J. Alloys Compd.* **2009**, *479*, L4–L7. [CrossRef]
116. Xiao, Q.; Yao, C. Preparation and visible light photocatalytic activity of Zn1−xFexO nanocrystalline. *Mater. Chem. Phys.* **2011**, *130*, 5–9. [CrossRef]